Dynamic Performance of High-Voltage Direct Current Systems for Offshore Wind Farm Based on Modular Multilevel Converter

MOHAMMED ABDELDJALIL DJEHAF
Department of Automatic Control, Faculty of Electrical Engineering,
Djillali Liabes University, Sidi Bel-Abbes, ALGERIA

YOUCEF ISLAM DJILANI KOBIBI
Department of Electrical Engineering, Faculty of Sciences and Technology,
Mustapha Stambouli University, 29000 Mascara, ALGERIA

MOHAMED KHATIR
Department of Automatic Control, Faculty of Electrical Engineering,
Djillali Liabes University, Sidi Bel-Abbes, ALGERIA

Abstract: The modular multilevel converter (MMC), which is the foundation of voltage-source converter (VSC)-high-voltage direct current (HVDC), has received significant attention over the past ten years. As a result, the MMC has undergone extensive technical and operational improvements, making it an appealing option for achieving efficient renewable energy harvesting, particularly for offshore wind farms. This paper discusses the state-of-the-art control algorithms that are most effective for simulating large HVDC systems, including offshore wind farms. Moreover, a test system is suggested to show how well the selected techniques perform in practical scenarios. Overall, this work will serve as a helpful shortcut to relevant material that pertains to this research topic.

Keywords: Modular multilevel converter (MMC); High-voltage direct current (HVDC) system; Voltage-source converter (VSC); Offshore wind farm; Control

Received: July 28, 2022. Revised: June 21, 2023. Accepted: July 25, 2023. Published: August 29, 2023.

1. Introduction

Due to increased awareness of climate change and falling technology costs, renewable energies have received significant attention over the past few decades. As a result, they have undergone significant improvement. This increase in adoption has led to new challenges in power system operation, owing to the intermittent nature of renewable energy generation, particularly from wind and solar photovoltaics. A stronger wind velocity profile at offshore farms helps them produce more electricity, which is another reason why wind power plants have the greatest growth when compared to other renewable energies. However, the deployment of onshore wind farms is constrained by construction limitations. The doubly fed induction generator (DFIG), which provides dynamic reactive power regulation, is most frequently used in modern offshore wind farms to power wind turbines with changing speeds. This system will provide independent regulation of active and reactive power when coupled to voltage source converters (VSCs), and it will rely on fast-switching transistors to avoid generating harmonic currents that could significantly impact the voltage waveform [1].

The future offshore wind farms will get larger and farther from the onshore grid as the supply of shallow water sites decreases. This inspires the development of unique and inventive offshore foundations that provide access to deeper water and maximize the market for offshore wind energy. The DolWin2 project, which is connected to an HVDC onshore station by a 90 km long land cable and an additional 45 km long DC sea cable system, is a fantastic example of what offshore wind farms in the future will typically look like. The 320-kV converter station, which has a 916 MW power transmission capacity, is also located on an offshore platform [2-4]. However, the above constraints will make HVAC transmission systems ineffective and problematic, particularly because of frequency and voltage instability and large charging currents of submarine cables [5]. This will encourage one alluring alternative that comes to overcome these problems: a point to point (P2P) VSC-HVDC system [6-7] capable of supplying weak grids or passive networks. For offshore applications, the VSC-HVDC system's black start capability and compact substation layout are crucial, in addition to autonomous, quick control of both active and reactive power flows.

The modular multilevel converter (MMC) [8] brings the VSC-HVDC transmission system to a higher level, thanks to such features as scalable modularity for higher voltages [9], low switching losses, low transient peak voltages [10], and lower harmonics content (high-quality AC voltage). This topology boasts better balancing capability than conventional voltage-source converters (VSCs), owing to the redundant combination of module connections for each required AC level [11]. It enhances imbalanced operation performance, improves symmetrical AC faults, and considerably lowers the probability of device and system failure [12].

This study offers a test system for evaluating the operational and control aspects (normal operation/dynamic performance) of a possible offshore wind farm connected to the onshore grid through a VSC-HVDC link based on 401 level MMC converters. The proposed control system, which consists of the upper-level control with its inner and outer control loops and the lower-level control with balancing control algorithm and modulation, is presented and described in details. The system is used to connect the offshore DFIG-based system. Next, various scenarios were simulated to investigate the effectiveness of the control system in normal operation and dynamic state through the step change.

Broadly speaking, this paper can be divided into three complementary sections: The first section briefly describes the DFIG and MMC systems. The second section gives an overview of the modular multi-level converter. The third section presents the simulated system and simulation results.

2. Literature Review

2.1 DFIG

The DFIG wind turbine has dominated the market for variable speed technology for models over 1.5 MW [13, 40-45]. The stator windings are coupled directly to the AC grid across the turbine transformer, whereas the rotor windings are connected to the grid via slip rings and a back-to-back (BtoB) voltage source converter (Figure 1).

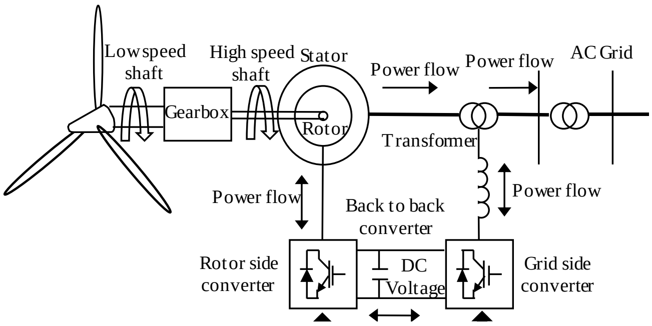

Fig. 1. Schematic diagram of a DFIG wind turbine

In comparison to fixed speed wind turbines, variable speed operation, made possible by the B2B converter and rotor blade pitch control, results in improved efficiency and higher energy yields. The B2B converter enables the wind turbine to operate at varied speeds by partially separating the mechanical and electrical frequencies of the rotor. Manwell et al. [14] and Nelson [15] described the main components of a DFIG wind turbine.

The rotor-side converter (RSC) and grid-side converter (GSC), which are connected by a shared DC bus, make up the two VSCs that constitute the B2B converter. While the GSC primarily maintains a constant DC voltage level on the B2B DC bus and offers, to some extent, reactive power support to the AC grid, the RSC controls the wind turbine speed and reactive power consumption by altering the rotor currents. The B2B converter is a rotor slip-power recovery device because the architecture of both converters permits bidirectional power transfer [25-29].

2.2 DFIGControl System

The primary variables that need to be managed in DFIG are the rotor speed, reactive power of the DFIG, DC voltage of the B2B converter, and reactive power of the grid side converter. Figure 2 displays a schematic diagram of the DFIG wind turbine's control loops.

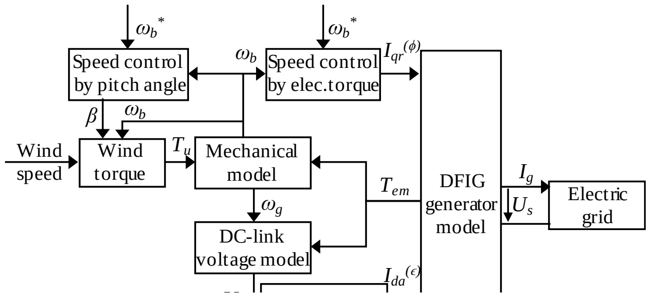

Fig. 2. DFIG models and control loop interaction

Both converter controllers [16] employ a feed-forward decoupled current control, the same as the receiving end converter (REC) of the VSC-HVDC. The pitch control pitches the rotor blades to minimize mechanical torque and restore the generator's rated speed when the wind speed exceeds its nominal value. The DIFG control system is fully described in previous literature [17-20].

3. Control Strategy

Three stages of a modular (n+1) level converter with n cells in each arm are depicted in Figure 3. In order to produce a multilayer voltage waveform at the converter terminal, this converter depends on the cell capacitors. Hundreds of cells are often required to build a single valve for DC transmission requirements. As the level count increases, the quality of the AC voltage waveform and the harmonic content both declines. Low dv/dt switching times and less voltage stress on the insulation of the interface transformers are produced by small voltage steps and a large number of SMs. As a result, it is not necessary to tolerate the DC link voltage or harmonic currents when using ordinary transformers. Further, switching losses and harmonic distortion are reduced as a consequence of the low effective switching frequency per device [29-33].

Because it is of the VSC type, the MMC topology requires an upper-level control more so than that of the preceding generation. Additional controllers are needed to govern internal variables (lower-level control): Now, the phase arms of the converter have series reactors built into them that regulate power flow and circulating currents, and each SM contains DC capacitors. Controlling these variables and injecting the modulation calls for the use of a balancing control algorithm (BCA) [21]. Figure 4 [22] depicts a high-level representation of the control structure.

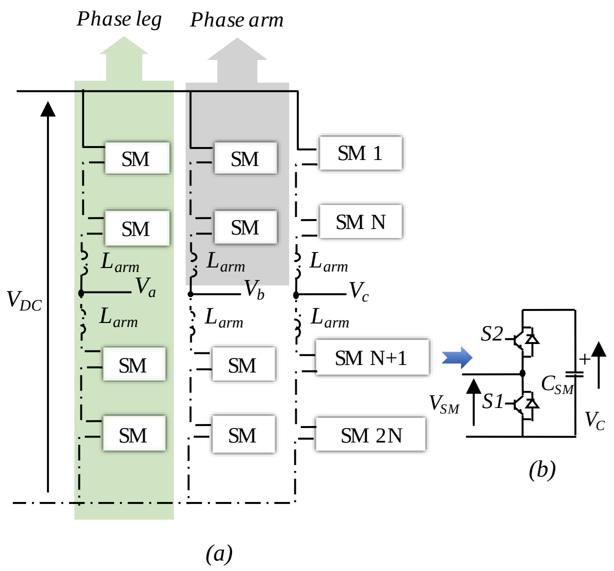

Fig. 3. (a) MMC converter topology, (b) Submodule configuration

The upper-level control block typically employs power angle and vector current controls. Power-angle control, also known as V/F control, is utilized when the VSC converter is linked to an AC system with a passive load or for wind turbine applications [22]. While the reactive power is regulated by modifying the VSC voltage magnitude, the active power is controlled by adjusting the phase angle shift between the VSC and the AC system [23].

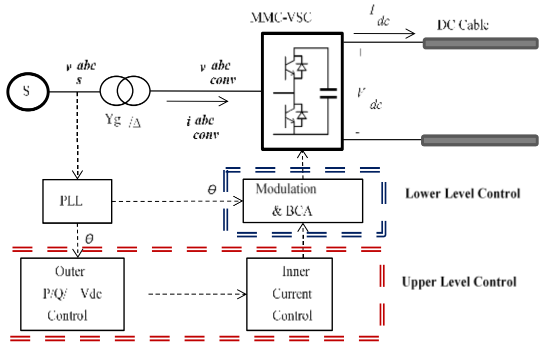

Fig. 4. Control hierarchy for the MMC station

The upper-level control block typically employs power angle and vector current controls. Power-angle control, also known as V/F control, is utilized when the VSC converter is linked to an AC system with a passive load or for wind turbine applications [22]. While the reactive power is regulated by modifying the VSC voltage magnitude, the active power is controlled by adjusting the phase angle shift between the VSC and the AC system [23].

Vector current control is a current control-based technology. When it notices disruptions, this control technique can immediately limit the current coming into the converter. Figure 4 illustrates the basic concept of vector-current control, which is to independently manage the instantaneous active and reactive power using a quick inner current control loop. Vector-current control for grid-connected VSCs has largely taken the place of alternative control schemes in practically all applications, owing to the successful implementation of the HVDC transmission system [23, 35-39, 42-45].

4. System Description

Figure 5 depicts a simplified single-line diagram of an offshore system. Up to 1,000 MW of offshore wind energy can be integrated by the MMC-HVDC system using a single core, 100 km undersea cable, which is modeled by a frequency dependent (wideband) model at 320 kV voltage. The onshore MMC is connected to a Thevenin comparable 400 kV, 50 Hz AC grid.

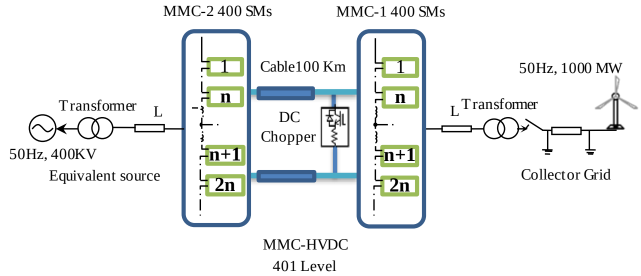

Fig. 5. MMC-HVDC 401 level HVDC connection of offshore wind farms to the transmission system

The EMTP-rv environment was selected to simulate the HVDC system of Figure 5, which is based on the switching function model and the nearest level control strategy. The simulated test cases assess the dynamic performance of the overall system of Figure 5 under various scenarios, including power flow operation and control strategy.

5. Performance Analysis

Several simulations were carried out to understand the operations of the previously discussed MMC converter-based wind power evacuation system. The dynamic performance of the transmission system was verified by simulating the normal operation of the HVDC connection of offshore wind farms to the transmission system, and by simulating the dynamic responses to step change applied to the reactive power regulator and DC voltage regulator at MMC 2.

5.1 Case A

The active power produced by wind farms—666 1.5 MW—and exported from MMC1 (an offshore station) to MMC2 (an onshore station) are shown in Figure 6. During the 3s simulation interval, the power reference at MMC1 is set to -1 p.u. The DC voltage is adjusted to 640 kV (320 KV), and the MMC2 operates at unity power factor. The simulation adopts the constant active power and constant reactive power mode. The active power setting for MMC1 (rectifier) is 1,000 MW, and for MMC2 is -1000 MW. The MMC 1 operates in VAC/F control and continuous AC voltage mode (inverter). The reactive power is maintained at 0 MVAr in MMC 2.

Initial settings for the offshore converter are for it to operate at maximum active power and absorb 150 MVAr. Figures 6 demonstrates that the converter can meet the required reactive power demands specified in the grid code and that the MMC-HVDC link can respond to the power demands of the wind farm (leading and lagging power factor of 0.95). Only the average capacitor voltage of each arm is presented for clarity in Figure 7, aiming to illustrate the capacitor voltages of the phase-a sub-modules of MMC 1 and MMC 2, which are kept balanced at their nominal values. The voltage imbalances within the converter's arm phases (upper and lower arm) lead to circulating currents with a second harmonic component. Thus, the phase voltages at the PCC for the onshore network (VAC1a) and the offshore network

(VAC1a) are shown to be almost sinusoidal and as such have a small harmonic content. This causes the SM capacitor voltages to ripple more and distorts the arm currents as well. Circulating currents can be stopped by placing a parallel capacitor (resonant filter) between the midpoints of the upper and lower arm inductances on each phase or by actively controlling the ac voltage reference. Smooth and stable DC voltages are therefore present.

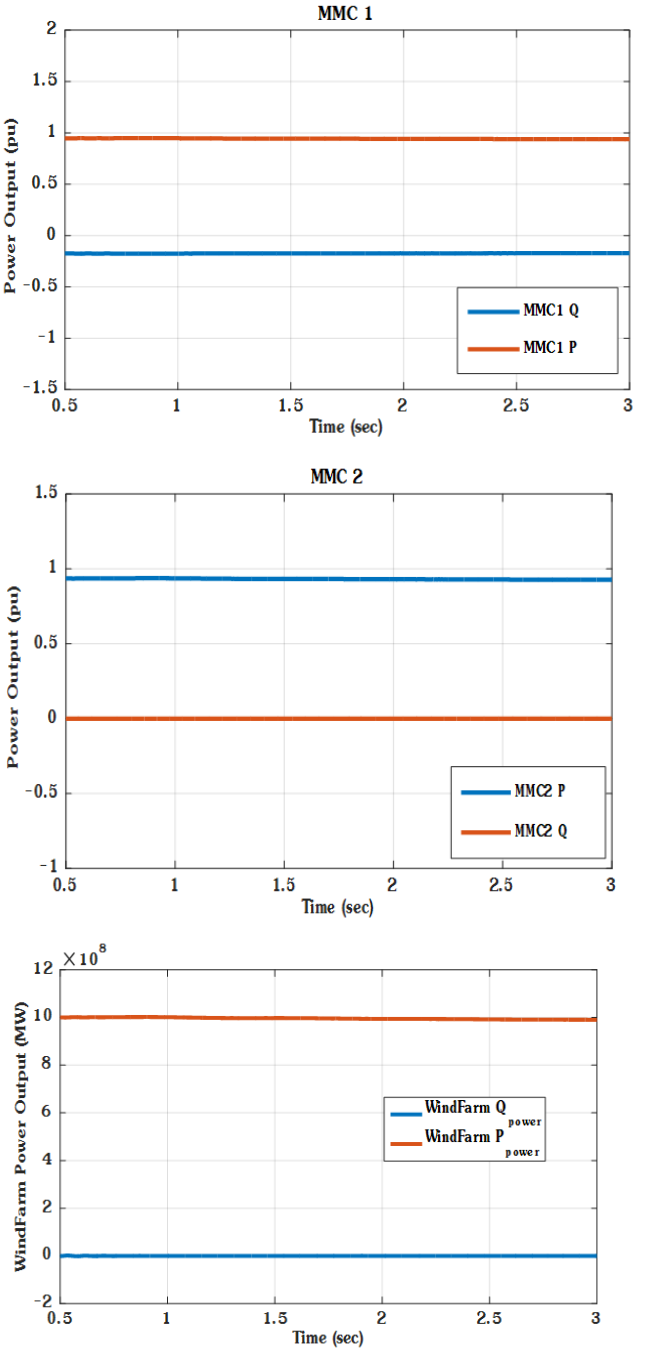

Fig. 6. Active and reactive power of HVDC connection and the offshore wind farms in normal operation

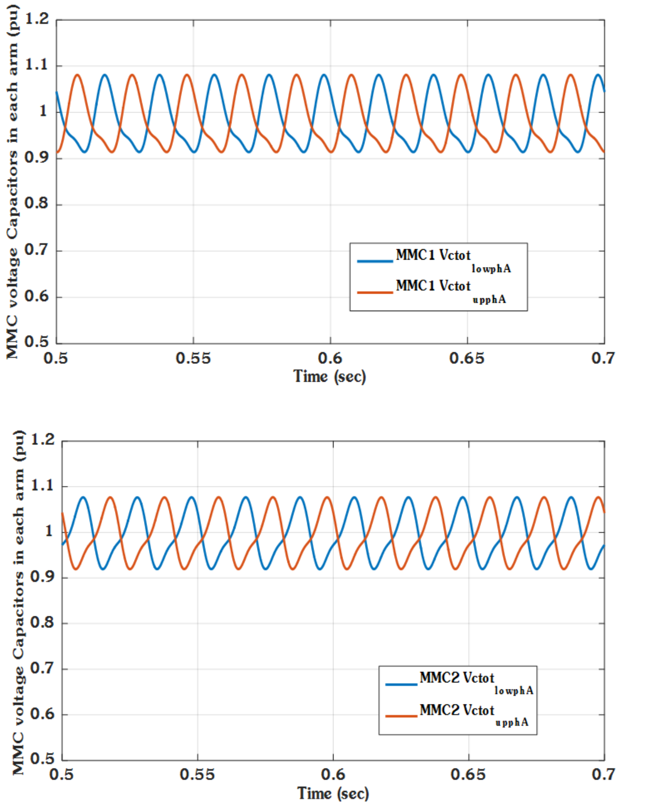

Fig. 7. Capacitor voltages of the phase-a sub-modules of MMC 1 and MMC 2 in normal operation

5.2 Case B

Two test cases were examined to assess the dynamic responses of MMC regulators. The reactive power order of MMC station 2 rose from 0 p.u. to 0.1 p.u. at t = 2 s. (onshore station), a sign of good tracking accuracy. The decoupling of the actual and reactive power control loops is confirmed by the fact that it is accomplished in 80 ms without compromising real power, as illustrated in Figure 8. Reactive power flow in each AC network can typically be separately controlled, and real power control is also independent. Figure 9 describes the response of the onshore MMC to a sudden drop in DC voltage order from 1 p.u to 0.9 p.u at t=2 s. It is accomplished without impacting reactive power in 50 ms. The active power experienced a transient due to this step change. It can also be observed from Figure 8 that the capacities of the arm remained balanced despite the decrease in the reference value to 0.9, by virtue of the direct relationship between the active power and the DC voltage.

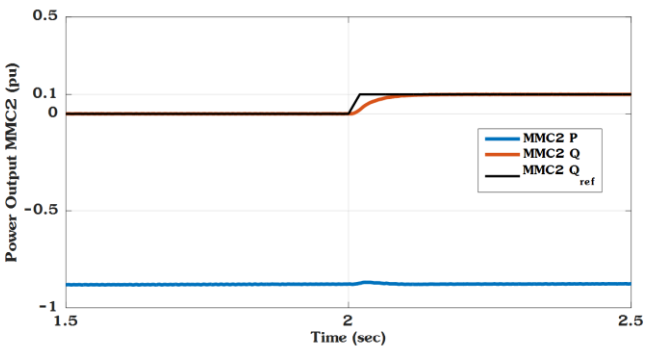

Fig. 8. HVDC system responses for reactive power step changes at MMC2

To evaluate the performance of the control system in both normal and dynamic operation, the two scenarios were tested through simulation. In the normal scenario, the offshore wind turbines' generated power will be efficiently transported to the onshore via the HVDC link. The step change simulation of the dynamic state helps to reveal the tracking accuracy, and assess the decoupled control of the active and reactive power and the DC voltage.

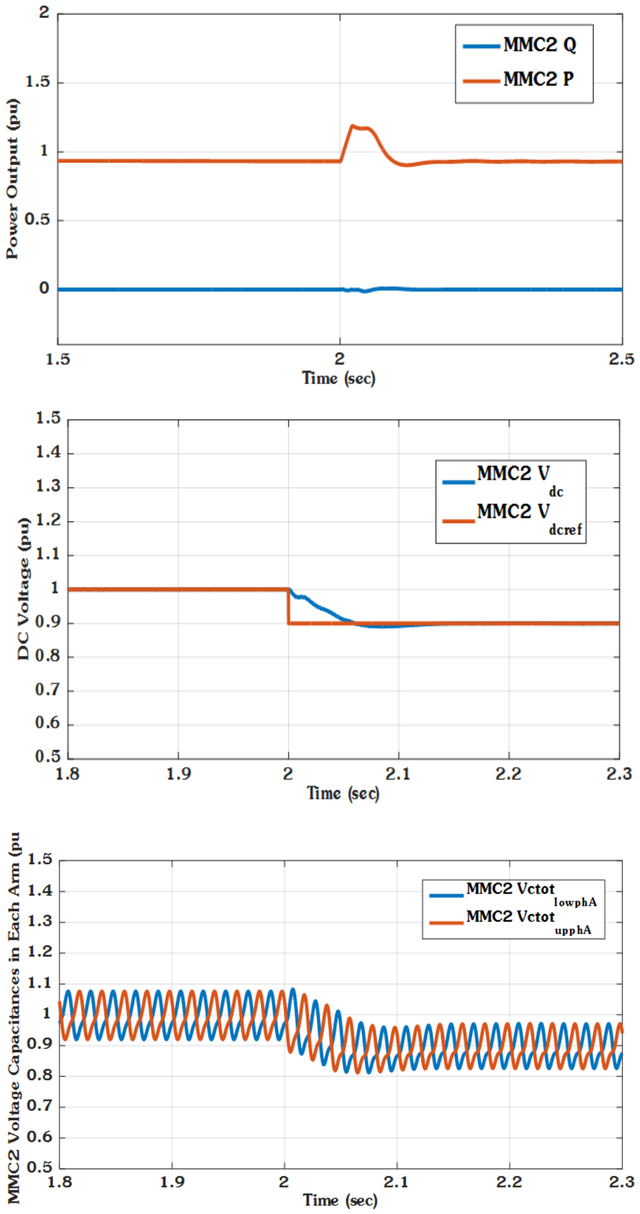

Fig. 9. HVDC system responses for DC voltage step changes at MMC2

6. Conclusions

This study carries out various simulations to evaluate the steady-state and dynamic performance of the MMC-HVDC link models, and presents the MMC control system and the components of the MMC-based HVDC. The simulation results are consistent with the control theory outlined above. The links' capacity to react to reactive power demand was examined using the proposed models. The outcomes demonstrate that the models might satisfy the reactive power requirements.

With the aid of the EMTP-rv simulation environment, the simulations were carried out in the time domain. The research results show that, for HVDC system applications under balanced grid conditions, the MMC, based on well-designed controllers, gives the needed dynamic response. The simulation results further demonstrate that the balancing capacity algorithm (BCA) approach can balance the voltage of the MMC capacitors for both steady-state and dynamic operational conditions.

Likewise, compared to the multi-level and multi-module VSC arrangements, the MMC's inherent scalability makes it a considerably more intriguing option for HVDC system applications. The performance in unbalanced grid conditions, as well as under single and three phase faults, will be the subject of further study.

References

[1] J. O. Tande, G. Di Marzio, and K. Uhlen, System Requirements for Wind Power Plants [Online]. Available: System Requirements for Wind Power Plants (Miscellaneous)|ETDEWEB (osti.gov), Accessed on: Sep. 5, 2022.

[2] ABB, ABB installs world's most powerful offshore converter platform in the North Sea, ABB, [Online]. Available: http://www.abb.com/cawp/seitp202/1FEB0F77B8682A0FC1257E9D002E4EF2.aspx, Accessed on: Jun. 5, 2022.

[3] Y. Chang and X. Cai, "Hybrid topology of a diode-rectifier-based HVDC system for offshore wind farms," *IEEE J. Em Sel Top. P.*, vol. 7, no. 3, pp. 2116-2128, 2019. https://doi.org/10.1109/JESTPE.2018.2881768.

[4] ABB, Largest offshore wind HVDC grid connection in the world [Online]. Available: https://library.e.abb.com/public/928326b06e04480ab0f216456bcf28ea/ABB_Flyer_TechDes_DolWin2_LR.pdf, Accessed on: Sep. 20, 2022.

[5] W. L. Kling, R. L. Hendriks, and J. H. Den Boon, "Advanced transmission solutions for offshore wind farms," in Power and Energy Society General Meeting-Conversion and Delivery of Electrical Energy in the 21st Century, Pittsburgh, PA, USA, July 20-24, 2008. https://doi.org/10.1109/PES.2008.4596257.

[6] G. P. Guo, H. F. Wang, Q. Song, J, Zhang, T. Wang, B. X. Ren, and Z. B. Wang, "HB and FB MMC based onshore converter in series-connected offshore wind farm," *IEEE T. Power. Electr.*, vol. 35, no. 3, pp. 2646-2658, 2020. https://doi.org/10.1109/TPEL.2019.2929689.

[7] B. Paola, L. K. Wil, L. H. Ralph, and V. Riccardo, "HVDC connection of offshore wind farms to the transmission system," *IEEE T. Energy Conver.*, vol. 22, no. 1, pp. 37-43. 2007. https://doi.org/10.1109/TEC.2006.889624.

[8] A. Lesnicar and R. Marquardt, "An innovative modular multilevel converter topology suitable for a wide power range," in Power Tech Conference Proceedings, Bologna, Italy, June 23-26, 2003. https://doi.org/10.1109/PTC.2003.1304403.

[9] B. Gemmell, J. Dorn, D. Retzmann, and D. Soerangr, "Prospects of multilevel VSC technologies for power transmission," in Transmission and Distribution Conference and Exposition, Chicago, IL, USA, April 21-24, 2008. https://doi.org/10.1109/TDC.2008.4517192.

[10] A. Silke, H. Roman, and M. Rainer, "New transformerless, scalable modular multilevel converters for HVDC-transmission," in 2008 IEEE Power Electronics Specialists Conference, Rhodes, Greece, June 15-19, 2008. https://doi.org/10.1109/PESC.2008.4591920.

[11] T. S. Gum, L. Hee-Jin, S. N. Tae, C. Yong-Ho, L. Uk-Hwa, B. Seung-Taek, H. Kyeon, and P. Jung-Wook, "Design and control of a modular multilevel HVDC converter with redundant power modules for noninterruptible energy transfer," *IEEE T. Power Deliver*, vol. 27, no. 3, pp. 1611-1619, 2012. https://doi.org/10.1109/TPWRD.2012.2190530.

[12] G. P. Adam, K. H. Ahmed, S. J. Finney, and B. W. Williams, "AC fault ride-through capability of VSC-HVDC transmission systems," in 2010 IEEE Energy Conversion Congress and Exposition, Atlanta, GA, USA, September 12-16, 2010. https://doi.org/10.1109/ECCE.2010.5617786.

[13] G. Paul, A. Lars, and J. Peter, Wind Energy-The facts Part I Technology, European Wind Energy Association, 2009 [Online]. Available: https://www.wind-energy-the-facts.org/part-i-technology.html, Accessed on: Jun. 5, 2022.

[14] J. Manwell, J. Mcgowan, and A. L. Rogers, *Wind Energy Explained: Theory, Design and Application*, Wind Engineering, vol. 30, no. 2, John Wiley & Sons, Ltd., 2010. http://dx.doi.org/10.1260/030952406778055054.

[15] V. Nelson, *Wind Energy: Renewable Energy and the Environment*, Taylor and Francis, 2009.

[16] R. Pena, J. C. Clare, and G. M. Asher, "Doubly fed induction generator using back-to-back PWM converters and its application to variable-speed wind-energy generation," *IEE P-Elect Pow. Appl.*, vol. 143, no. 3, pp. 231-241, 1996. https://doi.org/10.1049/IP-EPA%3A19960288.

[17] I. Erlich, J. Kretschmann, J. Fortmann, and S. Mueller-Engelhardt, "Modeling of wind turbines based on doubly-fed induction generators for power system stability studies," *IEEE T. Power Syst.*, vol. 22, no. 3, pp. 909-919, 2007. https://doi.org/10.1109/TPWRS.2007.901607.

[18] X. J. Liu and X. B. Kong, "Nonlinear model predictive control for DFIG-based wind power generation," *IEEE T. Autom. Sci. Eng.*, vol. 11, no. 4, pp. 1046-1055, 2014. https://doi.org/10.1109/TASE.2013.2284066.

[19] J. B. Hu, Y. B. He, and J. G. Zhu, "The internal model current control for wind turbine driven doubly-fed induction generator," in Conference Record of the 2006 IEEE Industry Applications Conference Forty-First IAS Annual Meeting, Tampa, FL, USA, October 08-12, 2006. https://doi.org/10.1109/IAS.2006.256525.

[20] H. X. Zong, C. Zhang, J. Lyu, X. Cai, M. Molinas, and F. Rao, "Generalized MIMO sequence impedance modeling and stability analysis of MMC-HVDC with wind farm considering frequency couplings," *IEEE Access*, vol. 8, pp. 55602-55618, 2020. https://doi.org/10.1109/ACCESS.2020.2981177.

[21] A. Antonopoulos, L. Angquist, and H. P. Nee, "On dynamics and voltage control of the modular multilevel converter," in 2009 13th European Conference on Power Electronics and Applications, Barcelona, Spain, September 08-10, 2009.

[22] D. Jovcic and K. Ahmed, *High Voltage Direct Current Transmission: Converters, Systems and DC Grids*, John Wiley & Sons Ltd, 2015, https://doi.org/10.1002/9781119566632.

[23] H. Saad, J. Mahseredjian, and S. Dennetière, Modular Multivel Converter in EMTP-RV, École Polytechnique de Montréal, Montréal, Canada, 2014.

[24] C. M. Ong, *Dynamic Simulations of Electric Machinery Using MATLAB/SIMULINK*, Prentice Hall PTR, 1998.

[25] I. Boldea, "The induction machine handbook," Taylor & Francis, 2020. https://doi.org/10.1201/9781003033417.

[26] R. Li, L. Yu, L. Xu, and G. P. Adam, "Coordinated control of parallel DR-HVDC and MMC-HVDC systems for offshore wind energy transmission," *IEEE J. Em. Sel. Top P.*, vol. 8, no. 3, pp. 2572-2582, 2020. https://doi.org/10.1109/JESTPE.2019.2931197.

[27] H. R. Fudeh and C. M. Ong, "Modeling and analysis of induction machines containing space harmonics Part I: Modeling and transformation," *IEEE T. Power Ap. Syst.*, vols. PER-3, no. 8, pp. 41-42, 1983. https://doi.org/10.1109/MPER.1983.5518874.

[28] A. Munoz and T. A. Lipo, "Complex vector model of the squirrel-cage induction machine including instantaneous rotor bar currents," *IEEE T. Ind. Appl.*, vol. 35, no. 6, pp. 1332-1340, 1999. https://doi.org/10.1109/28.806047.

[29] R. J. Kerkman, "Steady-state and transient analyses of an induction machine with saturation of the magnetizing branch," *IEEE T. Ind Appl.*, vols. IA-21, no. 1, pp. 226-234, 1985. https://doi.org/10.1109/TIA.1985.349684.

[30] J. Moreira and T. Lipo, "Modeling of saturated AC machines including air gap flux harmonic components," *IEEE T. Ind. Appl.*, vol. 28, no. 2, pp. 343-349. https://doi.org/10.1109/28.126740.

[31] W. Levy, C. F. Landy, and M. D. McCulloch, "Improved models for the simulation of deep bar induction motors," *IEEE T Energy Conver.*, vol. 5, no. 2, pp. 393-400, 1990. https://doi.org/10.1109/60.107238.

[32] W. Li, M. Zhu, P. Chao, X. Liang, and D. Xu, "Enhanced FRT and postfault recovery control for MMC-HVDC connected offshore wind farms," *IEEE T Power Syst.*, vol. 35, no. 2, pp. 1606-1617, 2020. https://doi.org/10.1109/TPWRS.2019.2944940.

[33] O. Thorsen, "Development and industrial application of a practical model for simulation of saturated deep bar induction machines," in Proceedings of 1994 IEEE Industry Applications Society Annual Meeting, Denver, CO, USA, October 02-06, 1994. https://doi.org/10.1109/IAS.1994.345487.

[34] S. I. Moon, A. Keyhani, and S. Pillutla, "Nonlinear neural-network modeling of an induction machine," *IEEE T. Contr. Syst. T.*, vol. 7, no. 2, pp. 203-211, 1999. https://doi.org/10.1109/87.748146.

[35] S. Sudhoff, D. Aliprantis, B. Kuhn, and P. Chapman, "An induction machine model for predicting inverter-machine interaction," *IEEE T Energy Conver.*, vol. 17, no. 2, pp. 203-211, 2002. http://dx.doi.org/10.1109/TEC.2002.1009469.

[36] M. Poller, "Doubly-fed induction machine models for stability assessment of wind farms," in 2003 IEEE Bologna Power Tech Conference Proceedings, Bologna, Italy, June 23-26, 2003. https://doi.org/10.1109/PTC.2003.1304462.

[37] Y. Z. Lei, A. Mullane, G. Lightbody, and R. Yacamini, "Modeling of the wind turbine with a doubly fed induction generator for grid integration studies," *IEEE T Energy Conver.*, vol. 21, no. 1, pp. 257-267, 2006. https://doi.org/10.1109/TEC.2005.847958.

[38] J. Ekanayake, L. Holdsworth, X. G. Wu, and N. Jenkins, "Dynamic modeling of doubly fed induction generator wind turbines," *IEEE T. Power Syst.*, vol. 18, no. 2, pp. 803-809, 2003. https://doi.org/10.1109/TPWRS.2003.811178.

[39] J. Ekanayake, L. Holdsworth, and N. Jenkinsb, "Comparison of 5th order and 3rd order machine models for doubly fed induction generator (DFIG) wind turbines," *Electr Pow. Syst. Res.*, vol. 67, no. 3, pp. 207-215, 2003. https://doi.org/10.1016/S0378-7796(03)00109-3.

[40] X. D. Liang and M. Abbasipour, "HVDC transmission and its potential application in remote communities: current practice and future trend," *IEEE T. Ind. Appl.*, vol. 58, no. 2, pp. 1706-1719, 2022. https://doi.org/10.1109/TIA.2022.3146117.

[41] W. S. Wang, G. H. Li, and J. B. Guo, "Large-scale renewable energy transmission by HVDC: Challenges and proposals," *Engineering*, 2022. https://doi.org/10.1016/j.eng.2022.04.017.

[42] H. Z. Li, J. Shair, J. Q. Zhang, and X. R. Xie, "Investigation of subsynchronous oscillation in a DFIG-based wind power plant connected to MTDC grid," *IEEE T. Power Syst.*, pp. 1-10, 2022. https://doi:10.1109/TPWRS.2022.3197185.

[43] Z. Din, J. Zhang, Z. Xu, Y. Zhang, A. H. Milyani, K. M. Cheema, A. Nawaz, and Y. Song, "Recent development and future trends of resonance in doubly fed induction generator system under weak grid," *IET Renew. Power Gener.*, vol. 16, no. 5, pp. 807-834, 2022. https://doi.org/10.1049/rpg2.12378.

[44] B. Yang, B. Q. Liu, H. Y. Zhou, J. B. Wang, W. Yao, S. C. Wu, H. C. Shu, and Y. X. Ren, "A critical survey of technologies of large offshore wind farm integration: Summary, advances, and perspectives," *Prot. Control Mod Power Syst.*, vol. 7, no. 17., 2022. https://doi.org/10.1186/s41601-022-00239-w.

[45] O. Boutfarjoute, H. Chekenbah, Y. Maataoui, and R. Lasri, "Grid stability: High penetration levels of renewable energies," in: Motahhir, S., Bossoufi, B. (eds) Digital Technologies and Applications, ICDTA 2022, Lecture Notes in Networks and Systems, Fez, Morocco, January 28-30, vol. 455, Springer, Cham. https://doi.org/10.1007/978-3-031-02447-4_60.

Contribution of Individual Authors to the Creation of a Scientific Article (Ghostwriting Policy)

The authors equally contributed in the present research, at all stages from the formulation of the problem to the final findings and solution.

Sources of Funding for Research Presented in a Scientific Article or Scientific Article Itself

No funding was received for conducting this study.

Conflict of Interest

The authors have no conflicts of interest to declare that are relevant to the content of this article.